J Physiol Sci (2011) 61:363–372
DOI 10.1007/s12576-011-0154-y

ORIGINAL PAPER

Protective effect of oxymatrine on chronic rat heart failure

Shu-Ting Hu · Ying Tang · Ya-Feng Shen · Hai-Hang Ao · Jie Bai · Yong-Liang Wang · Yong-Ji Yang

Received: 9 January 2011 / Accepted: 30 April 2011 / Published online: 22 June 2011

Abstract Oxymatrine is one of the alkaloids extracted from the Chinese herb *Sophora japonica* (*Sophora flavescens* Ait.) with anti-inflammatory, immune reaction inhibiting, antiviral, and hepatocyte and antihepatic fibrosis protective activities. However, the effect of oxymatrine on heart failure is not yet known. In this study, the effect of oxymatrine on heart failure was investigated using a Sprague-Dawley rat model of chronic heart failure. Morphological findings showed that in the group treated with 50 and 100 mg/kg of oxymatrine; intermyofibrillar lysis disappeared, myofilaments were orderly, closely and evenly arranged; and mitochondria contained tightly packed cristae compared with the heart failure group. We investigated the cytosolic Ca^{2+} transients and sarcoplasmic reticulum (SR) Ca^{2+} content, and assessed the expression of ryanodine receptor (RyR2), SR-Ca^{2+} ATPase (SERCA2a), and L-type Ca^{2+} channel (dihydropyridine receptor, DHPR). We found that the cytosolic Ca^{2+} transients were markedly increased in amplitude in the medium- ($\Delta F/F_0 = 26.22 \pm 2.01$) and high-dose groups ($\Delta F/F_0 = 29.49 \pm 1.17$) compared to the heart failure group ($\Delta F/F_0 = 12.12 \pm 1.35$, $P < 0.01$), with changes paralleled by a significant increase in the SR Ca^{2+} content (medium-dose group: $\Delta F/F_0 = 32.20 \pm 1.67$, high-dose group: $\Delta F/F_0 = 32.57 \pm 1.29$, HF: $\Delta F/F_0 = 17.26 \pm 1.05$, $P < 0.01$). Moreover, we demonstrated that the expression of SERCA2a and cardiac DHPR was significantly increased in the medium- and high-dose group compared with the heart failure rats. These findings suggest that oxymatrine could improve heart failure by improving the cardiac function and that this amelioration is associated with upregulation of SERCA2a and DHPR.

Keywords Oxymatrine · Heart failure · Sarcoplasmic reticulum · Ca^{2+} ATPase · L-type Ca^{2+} channel · Dihydropyridine receptor

Abbreviations

Ca^{2+}	Calcium
CICR	Ca^{2+}-induced Ca^{2+} release
DHPR	Dihydropyridine receptor
E-C coupling	Excitation-contraction coupling
HF	Heart failure
LTCC	L-type Ca^{2+} channel
NCX	Na^{+}–Ca^{2+} exchanger
OMT	Oxymatrine
PLB	Phospholamban
RyR	Ryanodine receptor
RyR2	Cardiac RyR
SERCA2a	SR-Ca^{2+} ATPase
SR	Sarcoplasmic reticulum

S.-T. Hu and Y. Tang contributed equally to the paper.

S.-T. Hu · J. Bai
Department of Physiology, Basic Medical Science College, Ningxia Medical University, 1160 Shengli Road, Yinchuan 750004, Ningxia, People's Republic of China

Y. Tang · Y.-F. Shen · Y.-L. Wang · Y.-J. Yang (✉)
Department of Biophysics, Second Military Medical University, 800 Xiangyin Road, Shanghai 200433, People's Republic of China
e-mail: husht@nxmu.edu.cn

H.-H. Ao
Department of Emergency, Affiliated Hospital of Ningxia Medical University, 804 Shengli Road, Yinchuan 750004, Ningxia, People's Republic of China

Introduction

Heart failure (HF) is characterized by a decline in the ability to pump the blood efficiently enough to meet the body's metabolic demands. The most common condition leading to heart failure is myocardial infarction; less frequently, heart failure is caused by valvular diseases, infections, and acquired or congenital cardiomyopathies. Heart failure is the leading cause of death in the Western world, and there is a lack of therapeutic agents that specifically target the underlying cellular defects [1].

A considerable amount of evidence in the literature suggests that the abnormal regulation of intracellular Ca^{2+} by the sarcoplasmic reticulum (SR) is an underlying mechanism of muscle dysfunctions in HF. It is generally agreed that much of the contractile dysfunction is caused by reduced myocyte calcium transients [2]. The SR Ca^{2+} content reflects the balance between Ca^{2+} uptake [by means of SR calcium ATPase (SERCA2a)] and Ca^{2+} efflux [by means of ryanodine receptors (RyRs)]. Therefore, a reduced SR Ca^{2+} content in heart failure may be due to reduced Ca^{2+} pumping by SERCA2a or increased SR Ca^{2+} leak by RyRs. Experimental evidence for both mechanisms has been reported in humans with heart failure and relevant animal models [3, 4]. In addition, reduced sarcolemmal Ca^{2+} influx (through L-type Ca^{2+} channels) [2] or enhanced cytoplasmic Ca^{2+} extrusion (by Na^{+}/Ca^{2+} exchange) may unload the SR [5]. In many cases of cardiac disease, altered Ca^{2+} cycling precedes the observed depression of mechanical performance, suggesting that an amelioration of the disorder of Ca^{2+} cycling will be the effective therapeutic strategy against heart failure [6].

Oxymatrine (OMT) is the major quinolizidine alkaloid from the root of *Sophora flavescens* Ait (kushen), which has long been used as a well-known traditional Chinese herb for the therapy of many diseases. The structure of OMT is clear, as shown in Fig. 1. Basic and clinical research has shown that OMT possesses a variety of pharmacological effects, such as immune system regulation, anti-inflammation, anti-apoptosis, anti-virus, anti-tumor, and anti-arrhythmic [7–13]. OMT also exerts a protective effect against ischemia or ischemia/reperfusion damage in the liver and intestine [14, 15].

The aim of this study was to investigate whether OMT has a cardioprotective effect in a rat model of chronic heart failure and the potential mechanisms for its cardioprotection.

Fig. 1 Chemical structure of oxynatrine

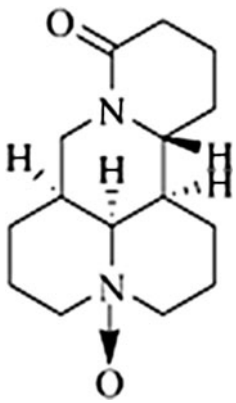

Materials and methods

Animals

Male Sprague-Dawley rats, weighing 200–250 g, were provided by the Second Military Medical University. The protocol was approved by the institutional animal care and use committee and the local experimental ethics committee. Rats were kept under a 12/12 h light/dark cycle and given free access to food and water. The animals were randomly divided into five groups ($n = 12$ for each group): the myocardial infarction (MI) group, high-dose group (rats with MI and 100 mg/kg OMT treatment), medium-dose group (rats with MI and 50 mg/kg OMT treatment), low-dose group (rats with MI and 25 mg/kg OMT treatment), and sham-operated group.

Surgical procedure

During the whole surgical period, the animals were randomized to receive either myocardial infarction (MI) [16] or a sham procedure. Rats were anesthetized by intraperitoneal injection of 10% chloral hydrate (3.5 ml/kg), cannulated, and ventilated with a tidal volume of 1.5–2 ml/100 g (80 strokes/min). A left lateral thoracotomy was performed between the third and fourth ribs, and the left anterior descending (LAD) coronary artery was permanently ligated proximally with a 5-0 silk suture. Sham-operated animals underwent the same procedure without ligation of the LAD. The chest was closed, the lung was reinflated, and the animal was moved to a prone position until spontaneous breathing occurred.

Drug administration

Oxymatrine injection (2 ml:0.6 g) was diluted in saline to prepare concentrations of 25 mg/ml. For the high-, medium-, and low-dose groups, OMT at doses of 100, 50, and 25 mg/kg (added with saline to a total volume of 1 ml), respectively, was administered by intraperitoneal injection and once daily on the following 28 days immediately after myocardial infarction. In the MI and sham-operated groups, an equal volume of saline was administered in the same manner.

Assessment of heart function

Twenty-eight days after MI, the rats were anesthetized with 10% chloral hydrate and placed on a pad. A micromanometer catheter was introduced into the right carotid artery and advanced across the aortic valve into the left ventricular cavity to record left ventricular pressures. Left ventricular end-diastolic pressure (LVEDP) and the maximum rates of contraction (d*p*/d*t*max) and relaxation (d*p*/d*t*min) were derived from the left ventricular pressure pulse [17]. Each hemodynamic evaluation was completed within 20–30 min. At the termination of the functional study, the heart was removed and its weight obtained.

Cell dissociation

Single cardiomyocytes (left ventricle cell) of the rat heart were isolated by an enzymatic dissociation method [18]. The heart was removed from the open chest of rats anaesthetized with 10% chloral hydrate and mounted on a modified Langendorff perfusion system for retrograde perfusion with Ca^{2+}-free Tyrode's solution; then the heart was perfused with a solution containing collagenase type II and bovine serum albumin (BSA) for about 8–10 min. After digestion, ventricular myocardium tissue was cut into small pieces in the modified Kraft-Bruhe (KB) solution [19] and gently shaken to dissociate cells. All experiments were conducted at room temperature (20–22°C).

Patch-clamp study

Whole-cell patch-clamp recordings of transmembrane ionic currents were performed with an EPC10 amplifier (HEKA Instruments, Germany). Cardiomyocytes were placed in a perfusion chamber. Patch electrodes were fabricated from borosilicate glass with a micropipette puller. Its resistance was 2–4 MΩ when the electrode was filled with the pipette solution. The potential of the electrode was adjusted to zero current between the pipette solution and the bath solution immediately before seal formation. After obtaining a gigaseal, a suction pulse was applied to establish the whole-cell mode. Command pulses were delivered and data were acquired with a patch-clamp amplifier controlled by the PULSE software connected to a computer. In the end, data analysis was performed.

Laser scanning confocal microscope analysis

Intracellular Ca^{2+} imaging was performed using a Leica TCS SP2 confocal microscope (Leica, Germany) in line-scan mode. Cytosolic Ca^{2+} measurement was performed using Fluo-3 Ca^{2+} indicators. When measured, Fluo-3 was excited by the 488-nm line of an argon-ion laser, and the fluorescence was acquired at wavelengths of 500–560 nm.

Patch-clamp and confocal microscope synchronous recording system software (researched and developed by our department) was used to record transmembrane Ca^{2+} currents ($I_{Ca \cdot L}$) and intracellular Ca^{2+} sparks simultaneously.

For quantitative studies, the temporal dynamics in fluorescence were expressed as $\Delta F/F_0 = (F - F_0)/F_0$, where F represents fluorescence at time t and F_0 stands for baseline fluorescence.

Transmission electron microscopy

For transmission electron microscopy (TEM), the ventricle myocardial tissue of a SD rat cut into 1 mm × 1 mm × 1 mm samples was fixed and kept in 4% paraformaldehyde for 4 h at 4°C, and post-fixed in 1% osmium tetraoxide for 2 h at room temperature. Then the tissues were dehydrated by graded alcohol and acetone embedded with Epon812 resin. Semithin sections were cut and examined by light microscopy. Thin sections from representative areas were then cut using a LEICA EM UC6 (Leica, Austria), stained with uranyl acetate and lead citrate, and examined with a H-7650 transmission electronic microscope (Hitachi, Japan).

Real-time quantitative RT-PCR determination of Ca^{2+} handling genes

The mRNA levels of RyR2, SERCA2a, and DHPR were measured using real-time quantitative RT-PCR. Total RNA was extracted using the TRIzol reagent and purified to remove any contaminating genomic DNA by on-column DNase digestion. First-strand synthesis and real-time amplification were performed using the Platinum qRT-PCR

Table 1 Primer sets for real-time quantitative RT-PCR

Gene names	Forward primers	Reverse primers
RyR2	5′-TAACCTACCAGGCCGTGGAT-3′	5′-GCTGCGATCTGGATAAGTTCAA-3′
SERCA2a	5′-CTGGCCGACGACAACTTCTC-3′	5′-TGAGGTAGCGGATGAACTGCTT-3′
DHPR (Cav1.2)	5′-CATCTTTGGATCCTTTTTCGTTCT-3′	5′-TCCTCGAGCTTTGGCTTTCTC-3′
GAPDH	5′-TGGAGTCTACTGGCGTCTT-3′	5′-TGTCATATTTCTCGTGGTTCA-3′

ThermoScript One-Step System (Invitrogene) and with the TaqMan Assays-on-Demand primer/probe pairs specific for RyR2, SERCA2a, DHPR, and GAPDH (glyceraldehyde-3-phosphate dehydrogenase). Standard amplification curves were generated from GAPDH. Optimal PCR curves were observed within 40 cycles using the real-time quantitative PCR system (FTC2000, Canada). Three sets of RNA isolations were evaluated, and each measurement was performed in triplicate. The threshold value (Ct) was set with the amplification-based threshold algorithms from Stratagene. GAPDH expression of each sample was used as endogenous control. All primer sets are listed in Table 1.

Western blotting

The levels of RyR2, SERCA2a, and DHPR proteins were determined by immunoblot analysis. Cell lysate proteins (500 μg) were subjected to SDS 4–8% PAGE. The SDS/PAGE-resolved proteins were transferred to nitrocellulose membranes. The nitrocellulose membranes containing the transferred proteins were blocked for 1 h with PBS containing 0.5% Tween 20 and 5% (w/v) skim milk. The blocked membranes were then incubated with antibody (1:1,000) (Wehrens XH 2003) for 1 h and washed three times for 5 min in PBS containing 0.5% Tween-20. The membrane was then incubated with the appropriate horseradish peroxidase-conjugated secondary antibody (1:5,000) for 1 h. After washing three times for 5 min each in PBS containing 0.5% Tween 20, these proteins were detected by enhanced chemiluminescence (ECL). Band densities were quantified by using LabWorks4.6 software (PerkinElmer).

Drugs and solutions

Oxymatrine (catalog no.: H20057480) was purchased from Chia-tai Tianqing Pharmaceutical Co. Ltd. (China); Fluo-3/AM was purchased from Biotium; TRIzol reagent was purchased from Invitrogen Life Technologies (USA), Protein G PLUS-agarose (catalog number: sc-2002) and Normal Mouse IgG (catalog number: sc-2025) were purchased from Santa Cruz, RyR antibody (catalog no.: ab2827), SERCA2a antibody (catalog no.: ab2817) and DHPRα1 antibody (catalog no.: ab58552) were purchased from Abcam, and collagenase type II was purchased from Worthington (USA). All other reagents were purchased from Sigma (USA). The composition of the Ca^{2+}-free Tyrode's solution was (in mM) NaCl 135, KCl 5.4, $MgCl_2$ 1.0, NaH_2PO_4 0.33, glucose 5.0, and HEPES 5.0 (pH 7.3). The composition of the digestion solution was Ca^{2+}-free Tyrode's solution 25 ml, collagenase type II 15 mg, BSA 50 mg, and 72 mmol/l $CaCl_2$ 20 μl. The composition of the modified Kraft-Bruhe (KB) solution was (in mM) KOH 80, L-glutamic acid 50, KCl 30, taurine 20, KH_2PO_4 30, $MgCl_2$ 3, glucose 10, EGTA 0.5, and HEPES 10 (pH 7.3). The external solution contained (in mM) NaCl 133.5, CsCl 4.0, $CaCl_2$ 1.8, $MgCl_2$ 1.2, HEPES 10, and glucose 11.1 (pH 7.3). Patch pipettes were filled with a solution that contained (in mM) CsCl 120, TEA-Cl 10, Na_2ATP 5, $MgCl_2$ 6.5, Tris GTP 0.1, and HEPES 10 (pH 7.2).

Statistical analysis

Data were expressed as mean ± SE for all experiments. Statistical analyses were made with ANOVA followed by Student-Newman-Keuls test for individual comparisons of means. The statistical significance was set at $^{**}P < 0.01$ HF versus sham, $^{*}P < 0.05$ HF versus sham, $^{\Delta\Delta}P < 0.01$ medium-dose, high-dose versus HF, $^{\Delta}P < 0.05$ medium-dose, high-dose versus HF.

Results

Characterization of cardiac function

According to the experiment, the infarct size of rat heart is more than 40%, and postoperative mortality is 20% in the

Table 2 Assessment of cardiac function in different groups

	Sham	HF	OMT (L)	OMT (M)	OMT (H)
Number	12	12	12	12	12
BW (g)	218.2 ± 12.7	227.1 ± 11.1	220.5 ± 23.5	232.4 ± 17.3	236.6 ± 15.4
HW/BW (mg/g)	2.42 ± 0.27	4.39 ± 0.19**	4.16 ± 0.33	3.11 ± 0.28$^{\Delta}$	3.08 ± 0.15$^{\Delta}$
HR (beats/min)	427 ± 15	435 ± 19	418 ± 28	427 ± 26	419 ± 17
LVEDP (mmHg)	3.9 ± 1.3	8.2 ± 1.8**	7.9 ± 1.2	5.1 ± 1.5$^{\Delta\Delta}$	4.6 ± 1.1$^{\Delta\Delta}$
dp/dt_{max} (mmHg/s)	4,182.77 ± 209. 53	2,462.95 ± 218.13**	2,783.74 ± 251.12	3,794.17 ± 223.59$^{\Delta\Delta}$	3,815.57 ± 205.11$^{\Delta\Delta}$
dp/dt_{min} (mmHg/s)	−2,892.31 ± 245.17	−1,554.46 ± 174.68**	−1,668.62 ± 171.53	−2,515.71 ± 188.43$^{\Delta\Delta}$	−2,661.78 ± 202.42$^{\Delta\Delta}$

MI myocardial infarction, *BW* body weight, *HW* heart weight, *HR* heart rate, *LVEDP* left ventricular end-diastolic pressure, dp/dt_{max} maximum change in systolic pressure over time, dp/dt_{min} maximum change in the rate of relaxation over time. Data are presented as mean ± *SE* 1 mmHg = 0.133 kPa, ** $P < 0.01$ HF versus sham, * $P < 0.05$ HF versus sham, $^{\Delta\Delta}$ $P < 0.01$ medium-dose, high-dose versus HF, $^{\Delta}$ $P < 0.05$ medium-dose, high-dose versus HF

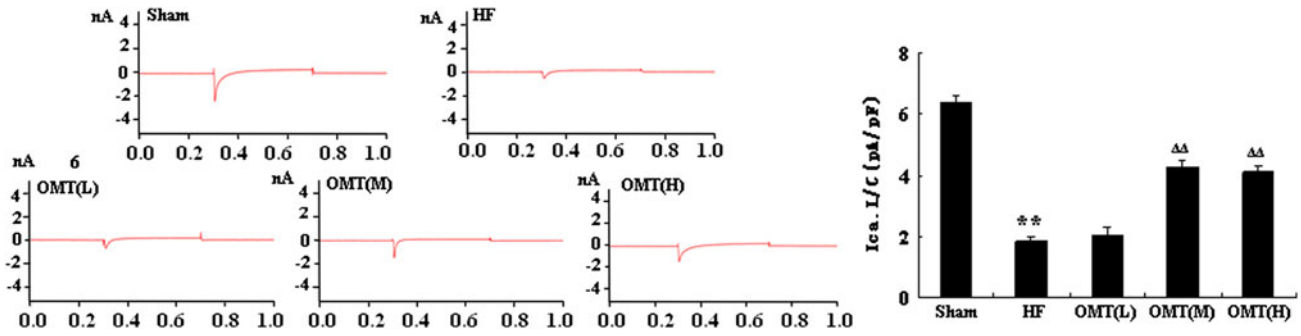

Fig. 2 Recordings of $I_{ca\bullet L}$ and the average current/capacitance (*p*A/*p*F) in different groups. The current was obtained in response to a 400-ms depolarizing step to +10 mV after a prepulse to −40 mV for 300 ms inactivated sodium current from a −40 mV holding potential

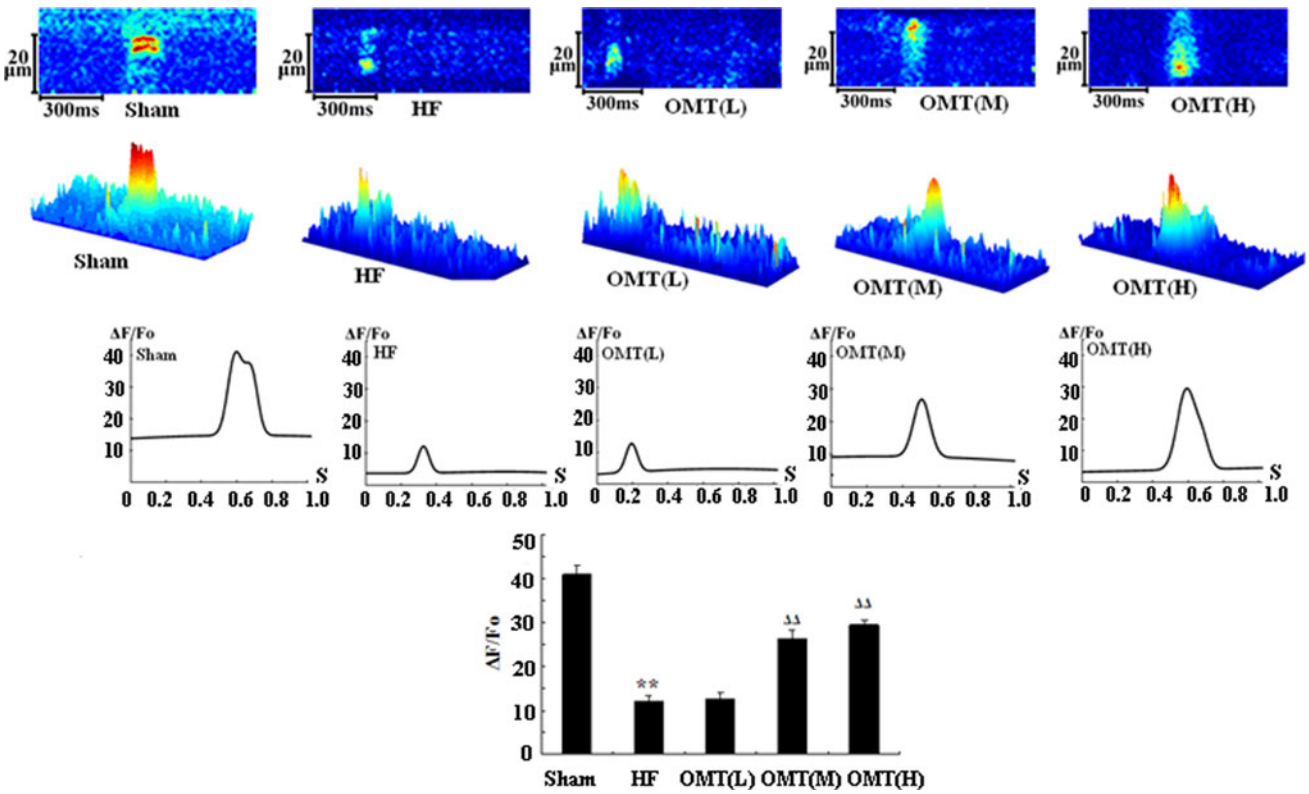

Fig. 3 Representative confocal line-scan images of $I_{ca\bullet L}$-induced Ca^{2+} transients, the spatial averages $I_{ca\bullet L}$-induced Ca^{2+} transients and the average amplitudes ($\Delta F/F_0$) of $I_{ca\bullet L}$-induced Ca^{2+} transients in different groups

HF group. Hemodynamic responses were assessed in different groups (Table 2). The maximum change in systolic pressure over time (dp/dt_{max}) was significantly increased by OMT at a dose of 50 mg/kg (3,794.17 ± 223.59 mmHg/s, $n = 12$) and 100 mg/kg (3,815.57 ± 205.11 mmHg/s, $n = 12$) versus the HF group (2,462.95 ± 218.13 mmHg/s, $n = 12$, $P < 0.01$). At a dose of 25 mg/kg, OMT increased the dp/dt_{max}, but did not reach a significant level. Furthermore, there was a significant decrease in heart weight (HW) divided by body weight (BW) in the medium-dose (3.11 ± 0.28, $n = 12$) and high-dose groups (3.08 ± 0.15, $n = 12$) compared with HF rats (4.39 ± 0.19, $n = 12$, $P < 0.01$), respectively.

Measurement of action potential-induced Ca^{2+} transients

Depolarization-induced long-lasting calcium current ($I_{Ca\cdot L}$) and spatially resolved intracellular Ca^{2+} transients (action potential-induced Ca^{2+} transients, ACT) were

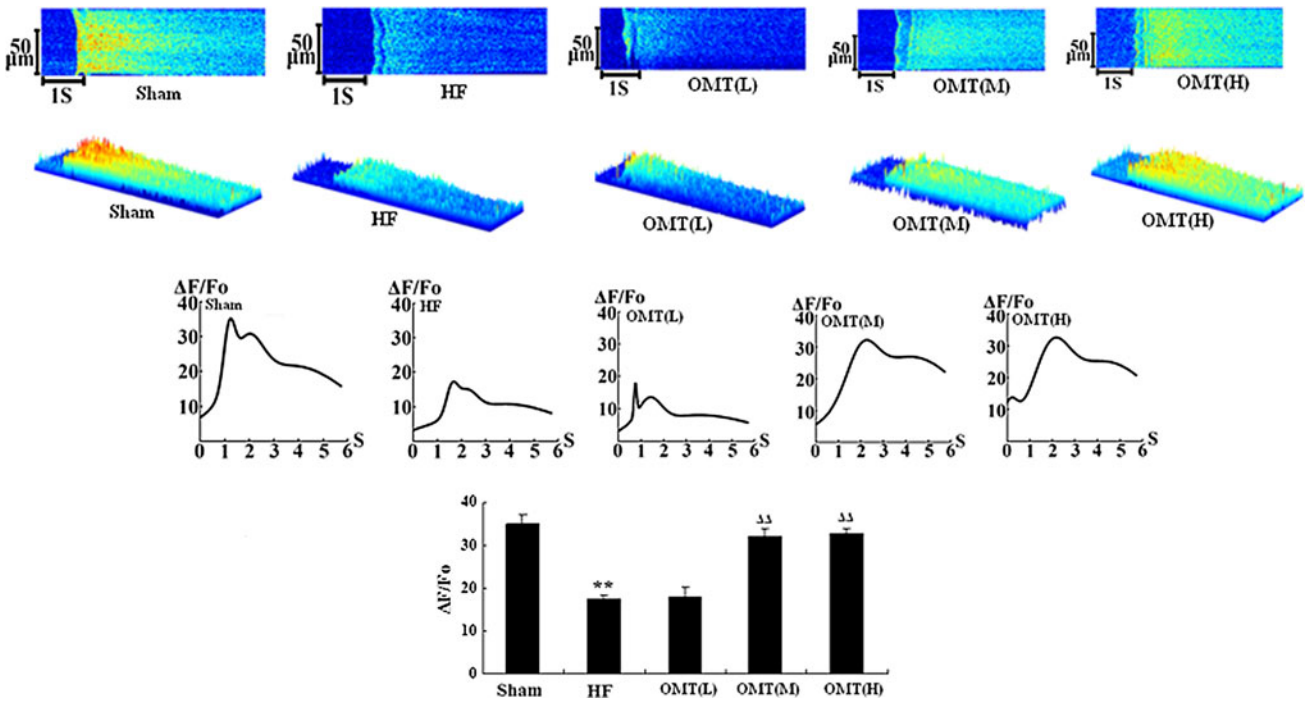

Fig. 4 Representative confocal line-scan images of caffeine-induced Ca^{2+} transients, the spatial averages of caffeine-induced Ca^{2+} transients, and the average amplitudes ($\Delta F/F_0$) of caffeine-induced Ca^{2+} transients in different groups

measured in cardiomyocytes dialyzed with Fluo-3/AM. They show representative traces of $I_{Ca \cdot L}$ and confocal line-scan images along with the spatial average of Ca^{2+} transients recorded during a depolarizing step from −40 to +10 mV in cardiac myocytes from different groups. The amplitude of $I_{Ca \cdot L}$ was increased in the medium- (4.25 ± 0.41, $n = 20$ cells from 10 medium-dose OMT-treated hearts) and high-dose groups (4.09 ± 0.32, $n = 20$ cells from 10 high-dose OMT-treated hearts) compared with the HF group (1.85 ± 0.14, $n = 16$ cells from 8 HF hearts, $P < 0.01$) (Fig. 2). Moreover the amplitude of Ca^{2+} transients was also increased in the medium- and high-dose groups. There was a significant increase in spatial averages ($\Delta F/F_0$) of $I_{Ca \cdot L}$-induced Ca^{2+} transients in the medium- (26.22 ± 2.01, $n = 12$ cells from 6 medium-dose OMT-treated hearts) and high-dose groups (29.49 ± 1.17, $n = 12$ cells from 6 high-dose OMT-treated hearts) compared with the HF group (12.12 ± 1.35, $n = 12$ cells from 6 HF hearts, $P < 0.01$) (Fig. 3).

Measurement of SR Ca^{2+} content

Isolated cardiomyocytes were loaded with Fluo-3/AM and rapidly perfused with caffeine (20 mM). SR Ca^{2+} content can be measured by caffeine-induced Ca^{2+} transients (CCT) during diastolic phase [20]. The images show that the amplitude of Ca^{2+} transients was increased in the medium- and high-dose groups. Caffeine-induced Ca^{2+} transients ($\Delta F/F_0$) were significantly increased in the medium- (32.20 ± 1.67, $n = 12$ cells from 6 medium-dose OMT-treated hearts) and high-dose groups (32.57 ± 1.29, $n = 12$ cells from 6 high-dose OMT-treated hearts) compared with the HF group (17.26 ± 1.05, n = 12 cells from 6 HF hearts, $P < 0.01$) (Fig. 4).

Observation under transmission electron microscopy

The ultrastructure of myocardial cells in the left ventricle of an SD rat was studied under TEM. In the control group, the myocardial cell appeared normal with intact sarcomeres; mitochondria contained tightly packed cristae. Numerous glycogen granules were present. In the HF group, some parts of the myocardial cell showed intermyofibrillar lysis and vesicles of varying size. Mitochondria were swollen, and mitochondrial cristae were separated. In the group treated with low-dose OMT, intermyofibrillar lysis had slightly improved, but a few mitochondria were still swollen, and mitochondrial cristae were separated. In the group treated with a medium dose of OMT, intermyofibrillar lysis disappeared; myofilaments were orderly, and closely and evenly arranged; and the mitochondria contained tightly packed cristae. The ultrastructure of myocardial cells treated with a high dose of OMT was similar to those of cells treated with a medium dose of OMT, and the electron density of some mitochondria increased (Fig. 5).

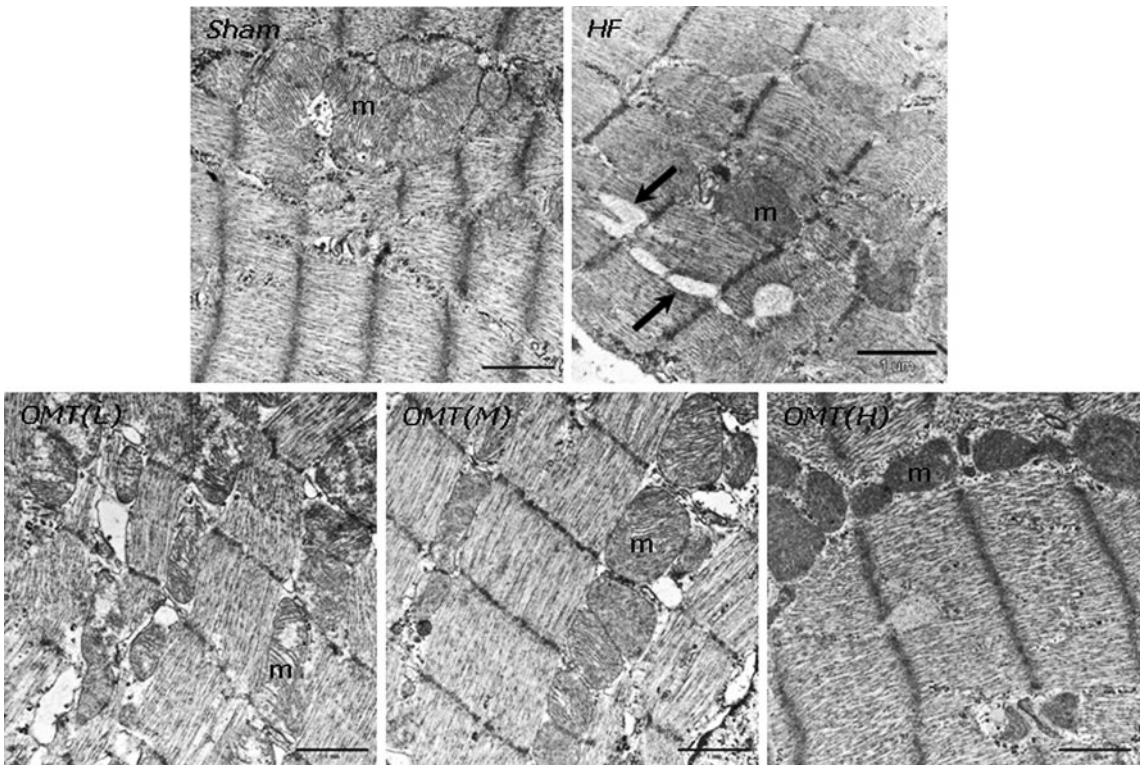

Fig. 5 The ultrastructure of myocardial cells in different groups. In the sham-operated group, the myocardial cell appeared normal with intact sarcomeres; mitochondria (m) contain tightly packed cristae. Numerous glycogen granules were present. In the HF group, some parts of the myocardial cell showed intermyofibrillar lysis (*arrows*) and vesicles of varying size; mitochondria were swollen, and mitochondrial cristae were separated. In the low-dose group, intermyofibrillar lysis improved slightly, but a few mitochondria were still swollen, and mitochondrial cristae were separated. In the medium-dose group, intermyofibrillar lysis disappeared; myofilaments were orderly, and closely and evenly arranged; and the mitochondria contained tightly packed cristae. The high-dose group was simular to that of the medium-dose group, and the electron density of some mitochondria increased (×30,000)

Effects of OMT on the mRNA expressions of Ca^{2+} handling genes

Real-time quantitative RT-PCR was performed to determine the relative mRNA expression pattern of RyR2, SERCA2a, and DHPR. We found that the mRNA expression of RyR2 failed to change in the medium- and high-dose group compared to the HF group ($P > 0.05$). The mRNA expressions of SERCA2a and DHPR were both increased in the medium- and high-dose groups compared to the HF group ($n = 8$, $P < 0.01$) (Fig. 6).

Effects of OMT on expressions of Ca^{2+} handling proteins

Immunoblot analyses were performed to determine the contents of the major SR Ca^{2+} handling proteins RyR2, SERCA2a, and DHPR in five groups. Compared with channel complexes from HF rat, the expression of RyR2 in the low-, medium-, and high-dose groups failed to change ($n = 6$, $P > 0.05$), whereas the SERCA2a content was significantly enhanced in the medium- and high-dose groups ($n = 6$, $P < 0.01$). Furthermore, the expression of DHPR was also increased in the medium- and high-dose groups ($n = 6$, $P < 0.01$) (Figs. 7, 8).

Discussion

HF is a chronic syndrome characterized by fatigue, peripheral edema, pulmonary congestion, and shortness of breath caused by a reduction in the ability of the heart to provide adequate blood flow to match the metabolic requirements of the organs. Defective intracellular Ca^{2+} homeostasis has been consistently reported in cases of heart failure [21, 22]. Because intracellular Ca^{2+} concentrations ($[Ca^{2+}]_i$) directly regulate the contractility of cardiomyocytes, a reduced $[Ca^{2+}]_i$ transient amplitude in heart failure results in decreased force development. A prolonged decay of the $[Ca^{2+}]_i$ transient and increased diastolic $[Ca^{2+}]_i$ may contribute to slowed relaxation of the failing heart [23, 24]. Several defects in the intracellular

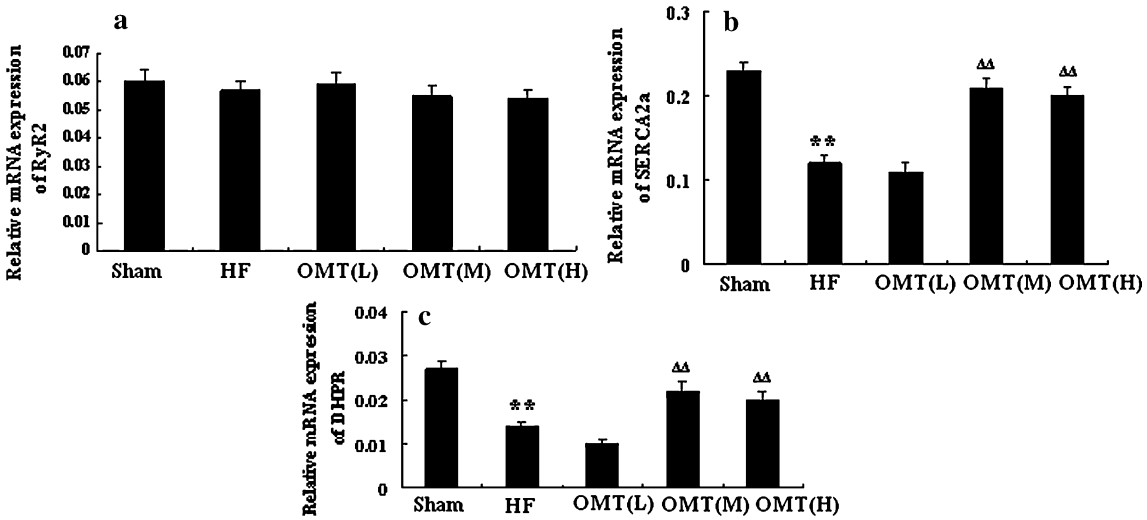

Fig. 6 Relative expression of Ca^{2+} handling genes RyR2 (**a**), SERCA2a (**b**), and DHPR (**c**) in the different groups ($n = 8$, $^{**}P < 0.01$ vs. sham group; $^{\Delta\Delta}P < 0.01$ vs. HF)

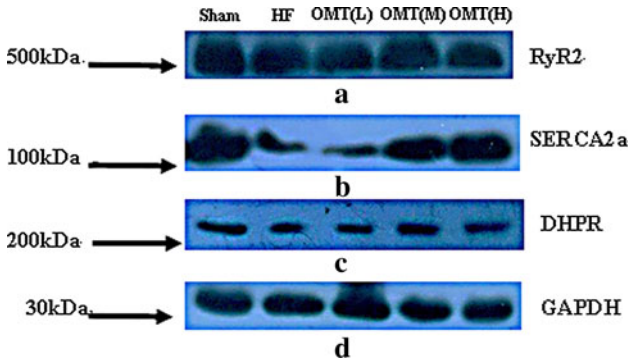

Fig. 7 Expression of RyR2 (**a**), SERCA2a (**b**), DHPR (**c**), and GAPDH (**d**) in the sham, HF, low-dose, medium-dose, and high-dose groups. *Arrows* on the left indicate the position of the molecular weight marker run in parallel to indicate protein migration on the gel

$[Ca^{2+}]_i$ metabolism have been reported, including depressed Ca^{2+} uptake, storage, and/or release of Ca^{2+} from the SR storage organelle [24–26]. Depressed SR Ca^{2+} release may result from decreased SR Ca^{2+} uptake via the SERCA2a, as well as a competitive increase of Ca^{2+} extrusion to the extracellular space via upregulated function of the plasma membrane Na^+/Ca^{2+} exchanger [23, 27]. Increased diastolic SR Ca^{2+} leak may also result in decreased SR Ca^{2+} loading and depressed contractility in HF [28, 29]. Diastolic SR Ca^{2+} leak is caused by "leaky" RyR2, which displays an increased sensitivity to Ca^{2+}-induced Ca^{2+} release and incomplete channel closure during diastole in heart failure [4].

Structural and functional alterations in the Ca^{2+} regulatory proteins present in the SR have recently been shown to play a crucial role in the pathogenesis of HF. Chronic activation of the sympathetic nervous system induces abnormalities in both the function and structure of these proteins. Both beta-blockers and angiotensin II receptor blockade (ARB) were found to suppress the hyperadrenergic state, thereby reversing PKA-mediated hyperphosphorylation of some proteins, such as the RyR2, restoring the FKBP12.6-mediated stabilization and inhibiting the Ca^{2+} leak.

Oxymatrine has been demonstrated to have a variety of pharmacological actions. Accumulating evidence indicates that oxymatrine may exert a protective effect on the cardiovascular system. Sun Hong-li et al. [30] have shown that administration of oxymatrine relieved myocardial injuries during ischemia, and this was achieved by protecting cardiomyocytes from apoptotic death. They have suggested that the beneficial effects of oxymatrine were likely mediated by an inhibition of lipid peroxidation (MDA production) and an increase in endogenous antioxidant activity (SOD), activation of the survival signaling molecule (Bcl-2), and a reduction of apoptotic mediator (Fas) and intracellular Ca^{2+} overload.

In the present study, we demonstrated that oxymatrine was a potent cardioprotective agent in ischemia-induced heart failure. Our data suggest that OMT may improve cardiac muscle function by reversing a maladaptive defect in intracellular Ca^{2+} signaling in heart failure. We found that administration of 50 mg/kg OMT was sufficient to provide significant cardioprotection against heart injury induced by myocardial infarction. We supported this finding by both functional (electrophysiological) and morphological data: increased Ca^{2+} transients (action potential-induced Ca^{2+} transients) and increased SR Ca^{2+} content (caffeine-induced Ca^{2+} transients), both of which are considered to be critical hallmarks of amelioration of heart failure. Our results showed that a series of morphological ameliorations was observed under electron

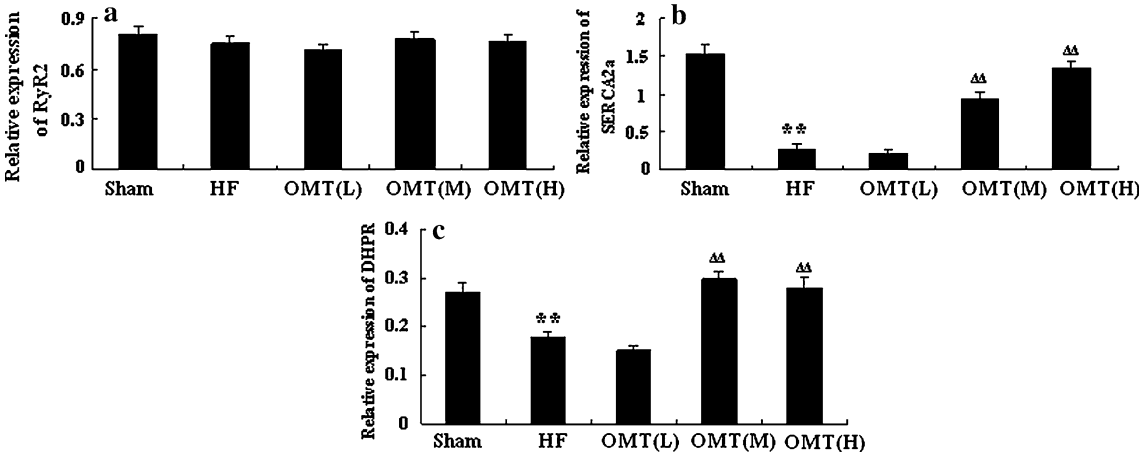

Fig. 8 Relative amount of Ca^{2+} handling proteins RyR2 (**a**), SERCA2a (**b**), and DHPR (**c**) in the different groups ($n = 6$, $^{**}P < 0.01$ vs. sham group; $^{\Delta\Delta}P < 0.01$ vs. HF)

microscopy. In the groups treated with medium- and high-dose OMT, intermyofibrillar lysis disappeared; myofilaments were orderly, and closely and evenly arranged; and the mitochondria contained tightly packed cristae.

At a dose of 25 mg/kg, OMT had no significant protective effect, so the cardioprotective effect of OMT was dose dependent. The minimum effective dose of OMT may be between 25 and 50 mg/kg, and this needs further study.

Depolarization of the plasma membrane by an incoming action potential activates voltage-gated L-type Ca^{2+} channels (LTCC) in plasma membrane invaginations called T-tubules. In the heart, LTCC (DHPR) activation results in a plasma membrane Ca^{2+} influx current, which triggers RyR2 activation and SR Ca^{2+} release, referred to as CICR. The efficiency of the trigger (the size of the inward Ca^{2+} current) needed to cause Ca^{2+} release from the SR has been termed E-C coupling gain. In many cases of HF, the E-C coupling gain seems to be reduced by a functional defect in the LTCC, an increase in the space between the LTCC and RyR, a decrease in SR Ca^{2+}, and/or an abnormality in the channel-gating property of RyR. Not only the amount of Ca^{2+} released for a given Ca^{2+} release trigger, but also the rate of Ca^{2+} release may be important for the contractility of the myofilaments. The present study shows that the expression of DHPR seems to be increased in the medium- and high-dose groups compared to the HF group, which leads to the increased amplitude of $I_{Ca \cdot L}$ and the increased Ca^{2+} release (action potential-induced Ca^{2+} transients).

In mammalian cardiac muscle, the SR is the major source of the calcium that activates contraction. The SERCA2a has a prominent role in excitation-contraction coupling of cardiac muscle, as it induces relaxation by sequestering Ca^{2+} from the cytoplasm. The stored Ca^{2+} is in turn released to trigger contraction. Ca^{2+} reuptake via SERCA2a is significantly influenced by phospholamban (PLB), a protein that, in its unphosphorylated form, inhibits SERCA2a, while in the phosphorylated state it favors SERCA2a activity. We found in our study that the expression of SERCA2a was increased in the medium- and high-dose groups compared with the HF group, which could increase Ca^{2+} reuptake (increase Ca^{2+} content), reduce Ca^{2+} overload, and improve the contractile recovery. Further investigation is still needed to clarify the effect of OMT on PLB.

In China, pure oxymatrine injection has been available in hospitals for treatment of hepatitis and tumors for many years. However, it has not been used for heart failure in the clinic. Since our results indicate that oxymatrine prevents heart failure in rats, we hope that it can be used to treat heart failure, although further research should be carried out in more animal experiments before clinical trials.

In this study, we found for the first time that oxymatrine had a beneficial effect on heart failure in rats. Although details of the mechanism of oxymatrine remain to be unraveled, the present results suggest that oxymatrine improves heart failure by improving the cardiac function and that this amelioration is associated with upregulation of SERCA2a and DHPR. We suggest that OMT may be a novel, effective therapeutic drug for the treatment of heart failure.

Acknowledgments This work was supported by The National Natural Sciences Fund Project of China (NSFC) and, in part, by the National Program on Key Basic Research Projects (the 973 Program Project). We thank Dr. Jianfei Wang for her technical assistance, and Shan Xu and Xiaoyan Fan for providing valuable suggestions.

References

1. McKenzie DB, Cowley AJ (2003) Drug therapy in chronic heart failure. Postgrad Med J 79:634–642

2. Bers DM, Eisner DA, Valdivia HH (2003) Sarcoplasmic reticulum Ca^{2+} and heart failure: roles of diastolic leak and Ca^{2+} transport. Circ Res 93:487–490
3. Piacentino V 3rd, Weber CR, Chen X, Weisser-Thomas J, Margulies KB, Bers DM, Houser SR (2003) Cellular basis of abnormal calcium transients of failing human ventricular myocytes. Circ Res 92:651–658
4. Marx SO, Reiken S, Hisamatsu Y, Jayaraman T, Burkhoff D, Rosemblit N, Marks AR (2000) PKA phosphorylation dissociates FKBP12.6 from the calcium release channel (ryanodine receptor): defective regulation in failing hearts. Cell 101:365–376
5. Pogwizd SM, Bers DM (2002) Na^{+}/Ca^{2+} exchange in heart failure: contractile dysfunction and arrhythmogenesis. Ann NY Acad Sci 976:454–465
6. Houser SR, Margulies KB (2003) Is depressed myocyte contractility centrally involved in heart failure? Circ Res 92:350–358
7. Liu M, Liu XY, Cheng JF (2003) Advance in the pharmacological research on matrine. Zhongguo Zhong Yao Za Zhi 28:801–804
8. Ma L, Wen S, Zhan Y, He Y, Liu X, Jiang J (2008) Anticancer effects of the Chinese medicine matrine on murine hepatocellular carcinoma cells. Planta Med 74:245–251
9. Liu SX, Chiou GC (1996) Effects of Chinese herbal products on mammalian retinal functions. J Ocul Pharmacol Ther 12:377–386
10. Jiang H, Hou C, Zhang S, Xie H, Zhou W, Jin Q, Cheng X, Qian R, Zhang X (2007) Matrine upregulates the cell cycle protein E2F-1 and triggers apoptosis via the mitochondrial pathway in K562 cells. Eur J Pharmacol 559:98–108
11. Azzam HS, Goertz C, Fritts M, Jonas WB (2007) Natural products and chronic hepatitis C virus. Liver Int 27:17–25
12. Yamazaki M (2000) The pharmacological studies on matrine and oxymatrine. Yakugaku Zasshi 120:1025–1033
13. Zhang MJ, Huang J (2004) Recent research progress of antitumor mechanism matrine. Zhongguo Zhong Yao Za Zhi 29:115–118
14. Jiang H, Meng F, Li J, Sun X (2005) Anti-apoptosis effects of oxymatrine protect the liver from warm ischemia reperfusion injury in rats. World J Surg 29:1397–1401
15. Zhao J, Yu S, Tong L, Zhang F, Jiang X, Pan S, Jiang H, Sun X (2008) Oxymatrine attenuates intestinal ischemia/reperfusion injury in rats. Surg Today 38:931–937
16. Tanonaka K, Furuhama KI, Yoshida H, Kakuta K, Miyamoto Y, Toga W, Takeo S (2001) Protective effect of heat shock protein 72 on contractile function in the perfused failing heart. Am J Physiol Heart Circ Physiol 281:H215–H222
17. van Rooij E, Doevendans PA, Crijns HJ, Heeneman S, Lips DJ, van Bilsen M, Williams RS, Olson EN, Bassel-Duby R, Rothermel BA, De Windt LJ (2004) MCIP1 overexpression suppresses left ventricular remodeling and sustains cardiac function after myocardial infarction. Circ Res 94:e18–e26
18. Ohmoto-Sekine Y, Uemura H, Tamagawa M, Nakaya H (1999) Inhibitory effects of aprindine on the delayed rectifier K^{+} current and the muscarinic acetylcholine receptor-operated K^{+} current in guinea-pig atrial cells. Br J Pharmacol 126:751–761
19. Nakaya H, Tohse N, Takeda Y, Kanno M (1993) Effects of MS-551, a new class antiarrhythmic drug, on action potential and membrane currents in rabbit ventricular myocytes. Br J Pharmacol 109:157–163
20. Song LS, Wang SQ, Xiao RP, Spurgeon H, Edward GL, Cheng HP (2001) Beta-Adrenergic stimulation synchronizes intracellular Ca^{2+} release during excitation-contraction coupling in cardiac myocytes. Circ Res 88:794–801
21. Morgan JP, Erny RE, Allen PD, Grossman W, Gwathmey JK (1990) Abnormal intracellular calcium handling, a major cause of systolic and diastolic dysfunction in ventricular myocardium from patients with heart failure. Circulation 81:III21–III32
22. Beuckelmann DJ, Nabauer M, Erdmann E (1992) Intracellular calcium handling in isolated ventricular myocytes from patients with terminal heart failure. Circulation 85:1046–1055
23. Hasenfuss G, Schillinger W, Lehnart SE, Preuss M, Pieske B, Maier LS, Prestle J, Minami K, Just H (1999) Relationship between Na^{+}–Ca^{2+} exchanger protein levels and diastolic function of failing human myocardium. Circulation 99:641–648
24. Pieske B, Sutterlin M, Schmidt-Schweda S, Minami K, Meyer M, Olschewski M, Holubarsch C, Just H, Hasenfuss G (1996) Diminished post-rest potentiation of contractile force in human dilated cardiomyopathy. Functional evidence for alterations in intracellular Ca^{2+} handling. J Clin Invest 98:764–776
25. Gomez AM, Valdivia HH, Cheng H, Lederer MR, Santana LF, Cannell MB, McCune SA, Altschuld RA, Lederer WJ (1997) Defective excitation-contraction coupling in experimental cardiac hypertrophy and heart failure. Science 276:800–806
26. Hobai IA, O'Rourke B (2001) Decreased sarcoplasmic reticulum calcium content is responsible for defective excitation-contraction coupling in canine heart failure. Circulation 103:1577–1584
27. Hasenfuss G, Reinecke H, Studer R, Meyer M, Pieske B, Holtz J, Holubarsch C, Posival H, Just H, Drexler H (1994) Relation between myocardial function and expression of sarcoplasmic reticulum Ca^{2+}-ATPase in failing and nonfailing human myocardium. Circ Res 75:434–442
28. Shannon TR, Pogwizd SM, Bers DM (2003) Elevated sarcoplasmic reticulum Ca^{2+} leak in intact ventricular myocytes from rabbits in heart failure. Circ Res 93:592–594
29. Yamamoto T, Yano M, Kohno M, Hisaoka T, Ono K, Tanigawa T, Saiki Y, Hisamatsu Y, Ohkusa T, Matsuzaki M (1999) Abnormal Ca^{2+} release from cardiac sarcoplasmic reticulum in tachycardia-induced heart failure. Cardiovasc Res 44:146–155
30. Sun HL, Li L, Shang L, Zhao D, Dong DL, Qiao GF, Liu Y, Chu WF, Yang BF (2008) Cardioprotective effects and underlying mechanisms of oxymatrine against ischemic myocardial injuries of rats. Phytother Res 22:985–989